Numerical Analysis of Electric Double Layer Capacitors with Mesoporous Electrodes: Effects of Electrode and Electrolyte Properties

Dante A. B. Iozzo,[†] Michael Tong,[‡,§] Gang Wu,[‡] and Edward P. Furlani*[‡,§]

[†]Department of Physics, University at Buffalo, Buffalo, New York 14261, United States
[‡]Department of Chemical & Biological Engineering, University at Buffalo, Buffalo, New York 14260, United States
[§]Department of Electrical Engineering, University at Buffalo, Buffalo, New York 14260, United States

ABSTRACT: A theoretical study is presented of the behavior of electric double layer (EDL) supercapacitors constructed from mesoporous activated carbon electrodes. A three-dimensional (3D) computational model is developed to predict the equilibrium charge distribution within the supercapacitor as a function of key electrode and electrolyte properties. The model is based on the modified Poisson–Boltzmann (MPB) equation and takes into account the impact of critical device parameters, including the size of the ions, the bulk ion concentration, the field-dependent permittivity of the electrolyte, the specific surface area of the electrodes, and the applied voltage. A key feature of the MPB model is that it limits the accumulation of ionic charge at the electrode–electrolyte interface by accounting for the finite size of the ions. This provides more accurate predictions of capacitance than models based on a point charge approximation. The model is used to perform a systematic parametric analysis of device performance and quantify the relative impact of various parameters on the gravimetric capacitance. It is also used to compare the capacitance obtained using organic versus inorganic electrolytes. The analysis confirms that aqueous electrolytes are able to attain a higher capacitance and power density. The model can be adapted to analyze the effects of arbitrary electrode morphologies and a broad range of electrolyte properties. It provides unique insight into the internal physics of an electrochemical cell and is well suited for the rational design of novel EDL supercapacitors.
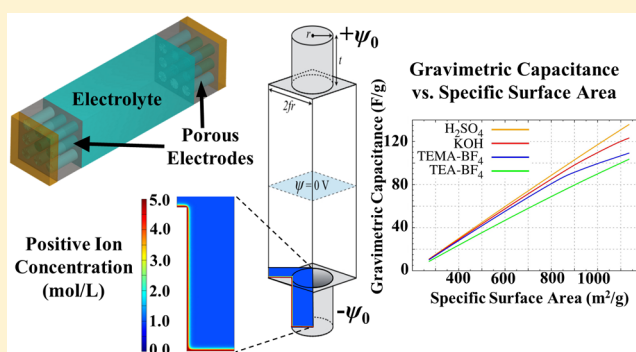
INTRODUCTION

In an electric double layer capacitor (EDLC) an electrolyte containing positive and negative ions is confined between an anode and cathode. The ions separate and accumulate on the surface of the oppositely charged electrodes in response to an applied voltage.[1−4] Energy is stored in an EDLC via the formation of the closely spaced layers of charge at the electrode–electrolyte interfaces.[1,5] The separation distance between the ions and the charged electrode can be considered as the distance between the "plates" of the capacitor. This minuscule separation, on the order of angstroms, coupled with the large surface area of highly porous activated carbon electrodes, enables EDLCs to have a significantly higher capacitance than traditional capacitors.[1−3] Moreover, physical storage of charge, instead of chemical storage, prevents the degradation of the electrochemical cells over nearly unlimited charge/discharge cycles.[5,6]

In addition, the charge and discharge time for EDLCs is on the order of a second, which provides a larger power density than traditional chemical batteries.[2,4] The breakdown of the electrolyte is a critical limiting factor in both the operating voltage and temperature of an EDLC. Water has a

decomposition voltage of 1.23 V, while organic solvents such as propylene carbonate (PC) and acetonitrile (AN) have a decomposition voltage of 2.7 V.[7,8] Thus, organic electrolytes are able to withstand higher operating voltages and therefore have a higher energy density than aqueous electrolytes. Aqueous electrolytes, however, are able to attain a higher power density.[4]

Despite the advantages and growing applications of EDLCs, many fundamental aspects of their performance are not well understood and rational design is lacking. To address these deficiencies, various groups have developed computational models to investigate the behavior of EDLCs and the impact of various design parameters on their capacitance. In one relatively popular simulation approach, the electrode–electrolyte interfaces of the supercapacitor are modeled using electrical circuit elements.[9] While this approach enables analysis of dynamic behavior, it lacks rigor, as it ignores critical physical details of the supercapacitor. Other more rigorous models have been

used to explore the effects of various carbon electrode morphologies on device performance. However, much of the previous work has been narrowly focused, with individual studies emphasizing relatively few select parameters.[2,5,6,8,10−15] Here, we apply rigorous methods to study EDLC behavior in a systematic fashion.

In this paper a 3D computational model is used to study the equilibrium behavior of EDL supercapacitors with mesoporous activated carbon electrodes as a function of key electrode and electrolyte properties. The model is based on the modified Poisson−Boltzmann (MPB) equation and is used to predict the equilibrium electrostatic potential within the EDLC, taking into account the finite size of the ions, electrode specific surface area, applied voltage, bulk ion concentration, and field-dependent permittivity of the electrolyte. The electric potential, in turn, is used to determine the EDLC charge distribution and capacitance. A key feature of the MPB model is that it limits the accumulation of ionic charge based on the packing of finite sized ions. This provides a more accurate prediction of device performance than simplified models that utilize a point charge approximation. A systematic analysis is performed to quantify the relative impact of the aforementioned parameters on the gravimetric capacitance. The largest impact on capacitance was obtained by varying the electrode specific surface area, followed in order of significance by the relative permittivity of the electrolyte, the hydrated ion diameter, and the bulk ion concentration. We found that the finite size of the ions played a significant role in the impact of other parameters, notably the bulk concentration. The model was also used to compare the capacitance obtained using organic versus inorganic electrolytes for a fixed EDLC configuration. This analysis confirms that aqueous electrolytes are able to attain a higher capacitance and thus a higher power density.

The model presented herein is readily implemented and computationally efficient, requiring less than an hour to complete a parametric analysis on a modern workstation. Moreover, it can be adapted to simulate EDLCs with arbitrary electrode morphologies and a broad range of electrolyte properties. The model provides unique insight into the internal physics of an electrochemical cell and is well suited for the rational design of novel EDL supercapacitors.

■ THEORY

Helmholtz Model. The concept of the supercapacitor was first theorized by Hermann von Helmholtz, who noticed that a layer of ions in a solution forms on an oppositely charged electrode.[1,16] He predicted that this layer of ionic charge, now known as the Helmholtz layer or Stern layer, adjacent to an oppositely charged electrode could be treated as a parallel-plate capacitor.[1] He further predicted that the capacitance of such a system would be inversely proportional to the thickness of the Helmholtz layer.[4] Helmholtz initially believed that the specific area capacitance was dependent neither on the electrolyte ion concentration nor on the surface potential, but this could not be demonstrated in practice.[17]

Gouy−Chapman Model. The dependence of the capacitance on electric potential and ion concentration was later developed by Gouy and Chapman independently.[13,14] They theorized that the electrolyte ions did not perfectly separate in solution forming a Helmholtz layer; rather, they conjectured that there was a continuous distribution of charge, with the highest concentrations of the ions occurring near the electrodes.[15] They created a model based on Maxwell−

Boltzmann statistics to take into account the ions' effect on each other. The Gouy−Chapman approach was accurate only for low surface charge densities at the electrode−electrolyte interface.[6]

Stern and BDM Models. In order to describe the behavior of the EDLC at high surface charge densities, Stern combined the two previous models: a Helmholtz layer at the electrode−electrolyte interface that transitions into a diffuse layer governed by Maxwell−Boltzmann statistics.[6,18] Grahame improved on the Stern model by inferring that the Stern layer actually has two different double layer thicknesses: an inner Helmholtz plane (IHP) and an outer Helmholtz plane (OHP). The IHP is formed by ions in direct contact with the electrode. The outer Helmholtz plane (OHP) is formed by ions in a solvation shell, a shell of polar solvent molecules that are attracted to the ion, increasing its effective radius. This solvation shell provides a layer of solvent molecules separating the ion and electrode.[6,19] Figure 1 illustrates the three models, detailing how the ions would behave according to each theory.
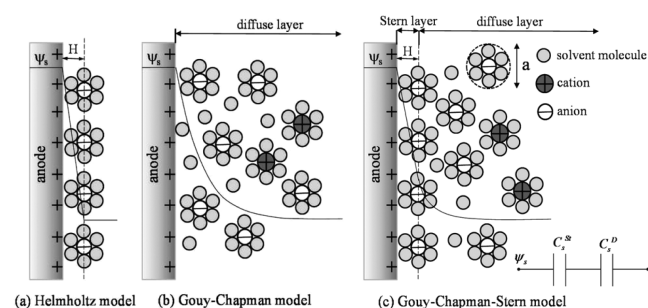
Figure 1. Previous models of the electric double layer.[1] The solvent molecules can be seen to form a solvation shell around the ions.

■ EQUILIBRIUM MODELS

Poisson−Boltzmann Equation. The equilibrium space charge density within an EDLC can be determined by solving a nonlinear Poisson−Boltzmann (PB) equation that relates the electrostatic potential ψ to the total ionic space charge,[6,15]

$$\nabla \cdot (-\epsilon_0 \epsilon_r \nabla \psi) = \mathcal{F} \sum_i Z_i c_i \tag{1}$$

where the summation is over the number of ionic species, ϵ_r is the relative permittivity of the solvent, $\mathcal{F}$ is Faraday's constant, Z_i is the valency of the ion, and c_i is the local ion concentration. The electric field within the EDLC can be recovered from the potential, i.e. $\mathbf{E} = -\nabla \psi$. Equation 1 needs to be solved self-consistently, as the ionic concentrations c_i depend on ψ. Specifically, from Maxwell−Boltzmann statistics we have,[15]

$$c_i = c_i^\infty \exp\left(\frac{-e Z_i}{k_B T} \psi\right) \tag{2}$$

where c_i^∞ is the bulk ion concentration, k_B is the Boltzmann constant and T is the temperature. The analysis simplifies considerably for EDLCs that utilize binary and symmetric electrolytes for which $i = 2$, $Z_1 = -Z_2 = Z$, and $c_1^\infty = c_2^\infty = c^\infty$. In this case, the PB equation reduces to the Gouy−Chapman (GC) equation:[15]

$$\nabla \cdot (-\epsilon_0 \epsilon_r \nabla \psi) = -2 \mathcal{F} Z c^\infty \sinh\left(\frac{e Z}{k_B T} \psi\right) \tag{3}$$

The GC equation has been solved analytically and can be linearized under the further assumption that the electrostatic energy imparted to the ions is far greater than their thermal energy.[15]

Modified PB Equation. The PB and GC equations both make the assumption that the ions are point particles.[6,11] However, the finite ion size can have an appreciable effect on the EDLC charge density, especially near the electrodes where the ions accumulate.[11] A key feature of the modified Poisson–Boltzmann (MPB) model, which distinguishes it from less rigorous models, is that it limits the accumulation of ionic charge based on the finite size of the ions. With the concentration determined by eq 2, a very high value of ψ would lead to a higher concentration than physically possible, i.e. one in which distinct ions physically overlap. By restricting the concentration, one can model the maximum packing for the Stern layer against the electrode. This can be achieved using the following expression for the concentration:[6,15]

$$c_i = \frac{c_i^\infty \exp\left(\frac{-eZ_i}{k_BT}\psi\right)}{1 + 2\nu_i \sinh^2\left(\frac{-eZ_i}{2k_BT}\psi\right)} \tag{4}$$

where $\nu_i = 2\,a_i^3 N_A c_i^\infty$ is a "packing" parameter, with N_A being Avogadro's number, relating how well the ions pack when forming the Stern layer. The parameter a_i is the hydrated diameter of the ion. By implementing eq 4 in eq 1, we arrive at the MPB equation for a general electrolyte that limits the accumulation of surface charge to a physically realizable concentration based on the physical size of the ions. In the case of a binary and symmetric electrolyte, the MPB equation can be further simplified to[5,6]

$$\nabla\cdot(-\epsilon_0\epsilon_r\nabla\psi) = -\mathcal{F}Zc^\infty \frac{2\sinh\left(\frac{eZ}{k_BT}\psi\right)}{1 + 2\nu\sinh^2\left(\frac{-eZ}{2k_BT}\psi\right)} \tag{5}$$

This version of the MPB was used in our model of the organic electrolytes, TEMA-BF$_4$ and TEA-BF$_4$, since both are binary and symmetric and have similar anion and cation sizes. The full MPB, eq 4 with eq 1, was used for the aqueous electrolytes H$_2$SO$_4$ and KOH.

■ ANALYSIS

Capacitor Configuration. The cell model of Varghese, Wang, and Pilon was employed in which the activated carbon electrodes are modeled as infinite thin sheets of finite thickness with a 2D array of highly ordered and identical cylindrical pores, cf. Figure 2.[6] The electrochemical cell has two oppositely facing and oppositely charged electrode arrays that are separated and arranged such that each pore in the anode is aligned with a pore in the cathode. The space between the electrodes is submicron and filled with the electrolyte. In this paper, the distance between the electrodes is chosen to be 140 nm. It should be noted that while we analyze electrodes with cylindrical pores, the model can be adapted to analyze arbitrary electrode morphologies and a broad range of electrolyte properties.

Due to the symmetry of the model, it is sufficient to simulate a unit cell of the electrode, which is defined by only one anode–cathode pore pair, cf. Figure 3. By setting the anode to a voltage ψ_0 and the cathode to $-\psi_0$, a plane of symmetry exists
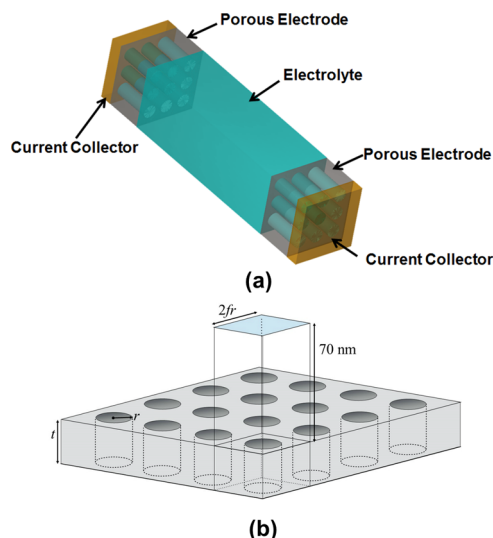
Figure 2. (a) Idealized capacitor with porous electrodes. (b) Activated carbon electrode modeled as an infinite sheet of finite thickness t inscribed with an array of highly ordered cylindrical pores.
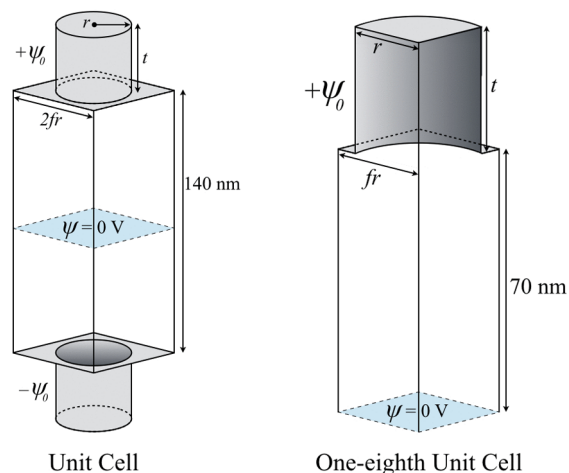
Figure 3. Schematic of a unit cell of the modeled supercapacitor, cf. Figure 2. The blue shaded plane between the anode and cathode pores is the plane of symmetry, held at $\psi = 0$ V. The gray shaded surfaces are the electrode–electrolyte interfaces, held at the value of the applied electrode voltage, ψ_0. The one-eighth unit cell can be used for binary and symmetric electrolytes with identical anion and cation sizes.

midway between the two electrodes where $\psi = 0$ V. One can reduce the computational complexity by further exploiting symmetry and dividing a unit cell into four equal parts. If the electrolyte is binary and symmetric, and if the anions and cations have the same hydrated diameter, then the charge distribution in the two sides of the electrolyte will only differ in the sign of the charge. Therefore, for such an electrolyte a one-eighth unit cell extending from one of the electrodes to the midplanes of symmetry is sufficient for simulation, cf. Figure 3. In this reduced model, the voltage in the midplanes is set to 0 V and the electrode–electrolyte interface is set to ψ_0, as shown. Symmetry or zero charge boundary conditions, $\mathbf{n}\cdot(\epsilon_0\epsilon_r\mathbf{E}) = 0$, are imposed on all other surfaces.

Each cylindrical pore has a radius r and a depth t. The thickness of the electrode is assumed to be slightly greater that the pore depth so that the outer surface of each electrode forms a conductive sheet. A factor of separation, f, is introduced to

define the spatial density of pores and hence the porosity of the electrode. Specifically, the length of the cross-sectional area of a square unit cell is $2fr$. Thus, as the porosity, ϕ, decreases, f increases. The volume of one of the electrodes in a unit cell, with the pore filled in, is $(2fr)^2t$. Since porosity is a ratio of the empty space to the total space, we can represent this as the ratio of an inscribing pore volume to the total volume of a unit cell electrode:

$$\phi = \frac{\pi r^2 t}{(2fr)^2 t} = \frac{\pi}{4f^2} \tag{6}$$

Thus, for example, a porosity of $\phi = 0.55$ corresponds to a separation factor of $f = 1.2$, which is reported to be a reasonable value for the porosity of activated carbon.[6] The cylindrical pore depth was set to $t = 30$ nm for all simulations.

While the majority of our analysis involves binary and symmetric electrolytes, we have also studied a triple species electrolyte consisting of aqueous sulfuric acid (H_2SO_4). In this case, it was necessary to model the full length of the cell (i.e., both the anode and the cathode), as there were no midplanes of symmetry due to the different ionic species having different charge and size. Nevertheless, it was still sufficient to model only a quarter of a unit cell that extended from the anode to the cathode.

Electrolytes. This study involves two popular choices of organic electrolytes, which are taken to be binary and symmetric: triethylmethylammonium tetrafluoroborate (TEMA-BF$_4$) dissolved in a solution of propylene carbonate (PC) and tetraethylammonium tetrafluoroborate (TEA-BF$_4$) dissolved in acetonitrile (AN).[6,8] This study also investigates two popular choices of aqueous electrolytes: potassium hydroxide (KOH) and sulfuric acid (H_2SO_4). The binary and symmetric electrolyte assumption is invalid for sulfuric acid, as it presents three species in solution: H_3O^+, HSO_4^-, and SO_4^{-2}. The simulations with 1 M sulfuric acid assumed a dissociation such that the concentrations of each species were 1 M H_3O^+, 0.988 M HSO_4^-, and 0.012 M SO_4^{-2}. All bulk ion concentrations were held constant in each simulation.

Field-Dependent Relative Permittivity. The permittivity within an electrolyte depends on the local electric field strength. This is especially important near a charged electrode where the spatial and orientational distributions of ions and molecules can produce a decrease in permittivity when the electrode surface charge density is sufficiently high.[20] This effect needs to be taken into account in order to obtain accurate predictions of capacitance. For example, it has been shown that the diffuse layer gravimetric capacitance predicted with a fixed (field-independent) permittivity can be twice that obtained using a field-dependent permittivity, with the latter more closely matching measured data.[6] In our analysis, we use the Booth model for the field-dependence of the relative permittivity as long as the electric field, E, is below 4×10^9 V/m:[5,6]

$$\epsilon_r(E) = n^2 + \frac{3}{\beta E}(\epsilon_r(0) - n^2)\left(\coth(\beta E) - \frac{1}{\beta E}\right) \tag{7}$$

where n is the index of refraction of the solvent and β is a coefficient dependent on the solvent molecule's magnetic dipole moment μ, the temperature T, and n:[5,6]

$$\beta = \frac{5\mu}{2k_BT}(n^2 + 2) \tag{8}$$

In order to successfully implement eq 7, one must make the replacement:

$$(\beta E) \rightarrow (\delta + \beta E) \tag{9}$$

where δ is a nonzero number small enough not to affect the value of $\epsilon_r(E)$ while preventing "dividing-by-zero" errors at $E = 0$ V/m. A value of $\delta = 10^{-8}$ was found to be reasonable and was used throughout our simulations. The value of the field-dependent relative permittivity at zero electric field strength, $\epsilon_r(0)$, is a property of the solvent.

Gravimetric Capacitance. The gravimetric capacitance, C_g, of an EDL supercapacitor is a key metric of its performance. This is given by[6]

$$C_g = \frac{A_{sp}}{\psi_0 A/Q + 1/C_s^{St}} \tag{10}$$

where A_{sp} is the specific surface area of the electrode, i.e. the intrinsic surface area per gram of bulk material. Also, ψ_0 is the applied electrode voltage, C_s^{St} is the Stern layer specific area capacitance, A is the surface area of the electrode–electrolyte interface, and Q is the total surface charge on surface A. In our analysis, we compute C_g using Q and A for the domain that we simulate. Thus, if a quarter unit cell is used, the electrode–electrolyte interface surface area for both electrodes is $A_{1/4} = 2f^2r^2 + \pi rt$. If a one-eighth unit cell model is used, A is the surface area of a quarter of an electrode pore (the gray surface in Figure 3), $2A_{1/8} = A_{1/4}$. For all of the simulations except the organic–inorganic electrolyte comparison, the electrode–electrolyte interface surface was fixed at $A_{1/8} = 615.2$ nm^2.

In eq 10, we can define the gravimetric capacitance solely due to the diffuse layer as[6]

$$C_g^D = \frac{Q}{\psi_0 A} \tag{11}$$

The surface charge Q is determined by integrating the surface charge density magnitude, $|\sigma(\mathbf{r})|$, over the electrode–electrolyte interface area:[6]

$$Q = \int_A |\sigma(\mathbf{r})| d^3\mathbf{r} \tag{12}$$

The specific surface area of the electrode is a characteristic of activated carbon, relating how much surface area per gram the substance has. Specific surface areas of carbon as high as 2400 m^2/g have been reported.[21] Using eq 6, one can derive the specific surface area from the surface area and mass, ρV, of the electrode. The volume, V, of a unit cell electrode is taken to be $t((2fr)^2 - \pi r^2)$. The amount of mass in a given volume of a porous electrode is $m_{p,e} = m(1 - \phi)$, where m is the mass of a nonporous electrode and ϕ is the porosity. Hence, the effective density of activated carbon, ρ, is actually $\rho_b(1 - \phi)$, where $\rho_b = 2.2$ g/cm^3 is the density of bulk graphite. Thus, we arrive at the equation for specific surface area of the electrode:[6]

$$A_{sp} = \frac{r + 2t\phi}{rt\rho_b(1 - \phi)} \tag{13}$$

■ RESULTS AND DISCUSSION

As noted above, the equilibrium supercapacitor analysis is based on the simplified MPB eq 5 for the symmetric organic electrolytes (TEMA-BF$_4$ and TEA-BF$_4$) and the full MPB, eq 1 for the nonsymmetric aqueous electrolytes (H_2SO_4 and KOH).

The equations were implemented using the COMSOL Multiphysics program (version 5.0, www.comsol.com), which employs a finite element-based solution method. The COMSOL electrostatics module with a stationary study and the direct PARDISO solver were used for this analysis. The simulations were run on two stand-alone multicore workstations.

An example of the equilibrium ion distribution for a symmetric electrolyte (i.e., one-eighth model) is shown in Figure 4. To ensure consistent results, mesh refinement was
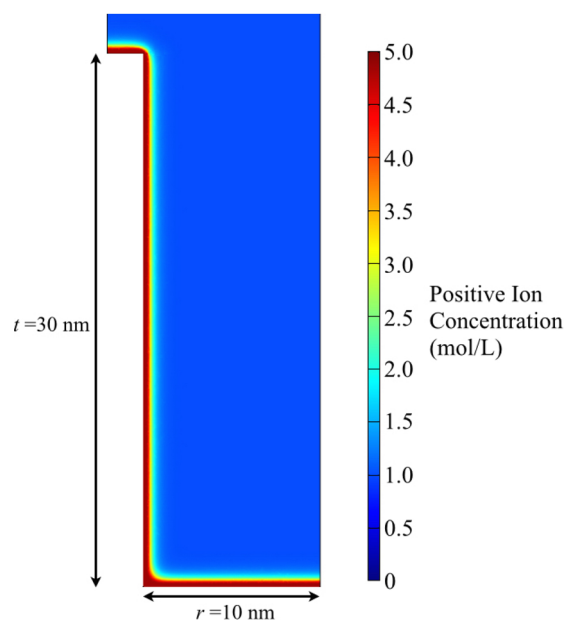
Figure 4. Cross-section of a simulated negative electrode pore for a one-eighth unit cell model (i.e., symmetric electrolyte) showing the equilibrium accumulation of positive TEMA$^+$ ions at the surface of the cathode. For a full pore, this cross section is mirrored across the boundary at the right.

maintained throughout all the computational results. The refinement chosen for the entire computational domain was a COMSOL predefined "extra fine" mesh, referring to a maximum computational element size of 3.5 nm, minimum element size of 0.15 nm, and resolution of narrow regions of 0.85, free tetrahedral calibration mesh. This mesh was coupled with a further refinement for the electrode−electrolyte interface boundaries. Each electrode boundary mesh was set to a maximum element size of 0.2 nm and a minimum element size of 0.04 nm.

Unless otherwise specified, the results discussed below are from a simulation of TEMA-BF$_4$ in a one-eighth unit cell with $\psi_0 = 1$ V and $c^\infty = 1$ M. The initial voltage within the cell was defined to be $\psi = 0$ V. The parameters for TEMA-BF$_4$ and the other three electrolyte species are listed in Table 1. It should be noted that our model was validated by successfully reproducing predictions reported in Varghese, Wang, and Pilon's study with a Stern layer capacitance of $C_s^{St} = 10 \ \mu F/cm^2$.[6]

Relative Permittivity. We computed the gravimetric capacitance as a function of $\epsilon_r(0)$ for both a field-dependent and fixed relative permittivity, as shown in Figure 5. While C_g increases with $\epsilon_r(0)$ in both cases, the field-dependent values are significantly lower than those obtained with a fixed permittivity.

Table 1. Model Parameters for the Four Electrolyte Species[a]

	TEMA-BF$_4$	TEA-BF$_4$	KOH	H$_2$SO$_4$
Solvent	PC	AN	H$_2$O	H$_2$O
a_- (nm)	0.70[6]	0.69[6]	0.662[22]	0.758[22]
a_+ (nm)	0.70[6]	0.69[6]	0.600[22]	0.560[22]
$\epsilon_r(0)$ at 298 K	64.4[6]	35.97[6]	78.39[23]	78.39[23]
n at 298 K	1.42[6]	1.34[6]	1.3325[24]	1.3325[24]
μ ($\times 10^{-30}$ Cm)			6.171[25]	6.171[25]
β ($\times 10^{-8}$ m/V)	1.314[6]	3.015[6]	1.416	1.416

[a]Both HSO$_4^-$ and SO$_4^{-2}$ were assumed to have the same hydrated radius.
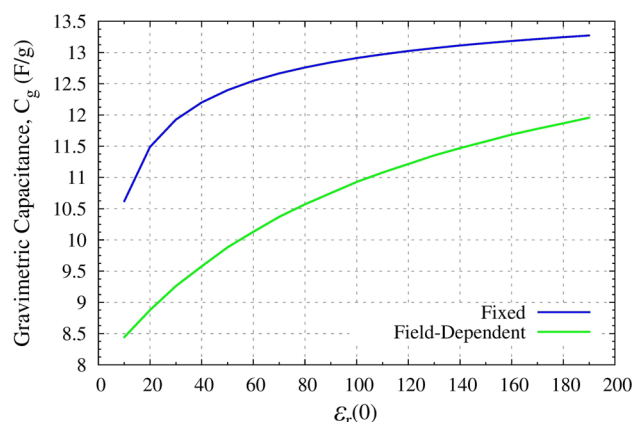
Figure 5. Gravitmetric capacitance as a function of $\epsilon_r(0)$. The relative permittivity was compared between the field-dependent model with $\epsilon_r(E)$ given by eq 7, and a fixed value with $\epsilon_r = \epsilon_r(0)$.

This can be understood by considering the functional dependency of ϵ_r as described by the Booth model eq 7, cf. Figure 6. Note that $\epsilon_r(E)$ decreases as E increases, and
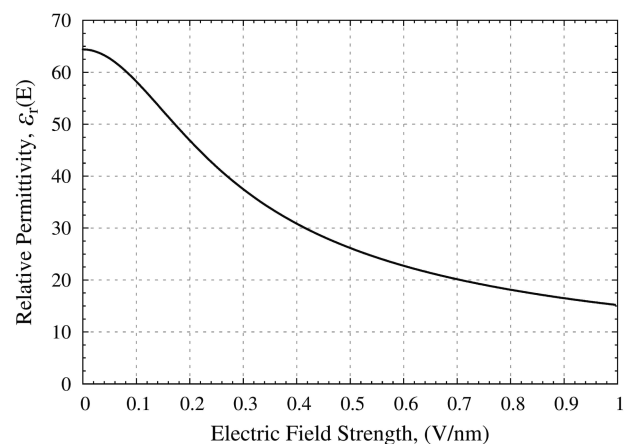
Figure 6. Field-dependent relative permittivity as a function of electric field strength, as governed by the Booth model, eq 7. The values of $\beta = 1.314 \times 10^{-8}$ m/V, $n = 1.42$, and $\epsilon_r(0) = 64.4$ were used.

therefore, the field-dependent permittivity will generally be lower than the fixed permittivity for a given value of $\epsilon_r(0)$. Thus, the predicted C_g at that value will be lower using $\epsilon_r(E)$ in eq 5. This is an important distinction, as predictions of C_g based on a field-dependent permittivity have been shown to provide a better fit to experimental data than those obtained with a fixed permittivity.[6]

Hydrated Ion Diameter. When studying the gravimetric capacitance as a function of hydrated ion diameter, the simulations show that the capacitance decreases appreciably as the ion diameter increases, as shown in Figure 7. Specifically,
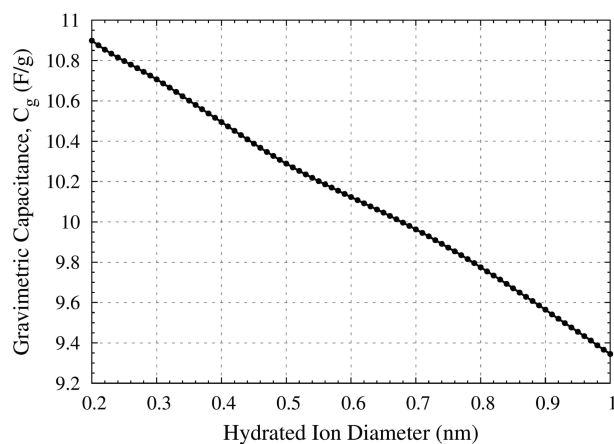
Figure 7. Gravimetric capacitance as a function of hydrated ion diameter for an organic electrolyte dissolved in PC. All other parameters were taken from TEMA-BF$_4$, cf. Table 1.

the gravimetric capacitance is inversely proportional to the hydrated ion diameter. This is due to the packing of the ions at the electrode−electrolyte interface. Larger ions are less densely packed than smaller ions, and this results in a lower surface charge density, which results in lower charge and hence lower capacitance, cf. eq 12. Thus, the bulk concentration should not affect this relationship, and this was confirmed as we obtained essentially the same plot in Figure 7 when we tripled the bulk concentration to 3 M.

Bulk Ion Concentration. Figure 8 shows the relationship between the gravimetric capacitance and bulk ion concen-
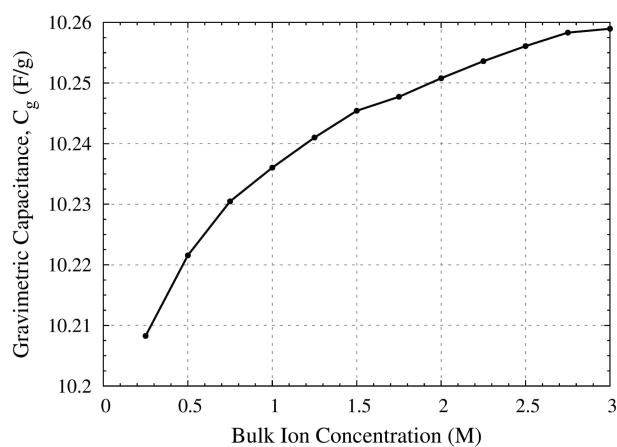
Figure 8. Gravimetric capacitance as a function of bulk ion concentration for TEMA-BF$_4$ in PC, an organic binary and symmetric electrolyte.

tration. While a positive correlation exists, the effect appears to be minimal. An increase in capacitance of less than half a percent is predicted as the concentration essentially triples from 1 to 3 M. This small increase diminishes further at higher concentrations. The minimal sensitivity to bulk concentration is due to a "saturation" of the number of charge carriers in the Stern layer. If the maximum number of ions that pack into the

Stern layer (based on the finite size of the ions) is achieved at relatively low concentrations, then any higher concentration will have a negligible contribution to the capacitance.

Electrode Surface Charge. We studied the equilibrium value of accumulated ionic charge density Q at the electrode− electrolyte interface as a function of the applied electrode voltage, ψ_0, over a range of 0 to 1.4 V. As shown in Figure 9, Q rises rapidly at low voltages but saturates as ψ_0 increases. This is due to the limitation imposed by the packing of finite sized ions.
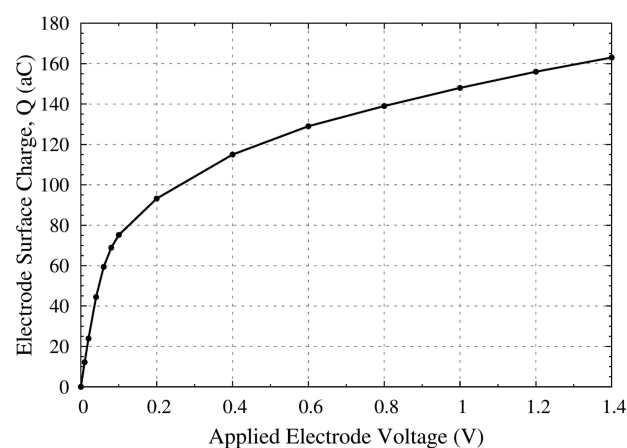
Figure 9. Accumulated surface charge density, Q, on the anode as a function of the applied voltage, ψ_0, clearly showing the rapid buildup of charge at low voltage. For $\psi_0 > 0.2$ V, the voltage becomes continually less effective at increasing surface charge.

Comparing Electrolytes. It has already been demonstrated[6] that the specific surface area of the electrode has the strongest impact on gravimetric capacitance, which our model confirms, cf. Figure 10. We use this relationship to compare the two most commonly used organic and inorganic electrolytes. The choice of using either an organic or inorganic electrolyte depends on the desired performance and purpose of the cell. Both organic electrolytes, TEMA-BF$_4$ and TEA-BF$_4$, have the benefit of being binary and symmetric, with the cation and
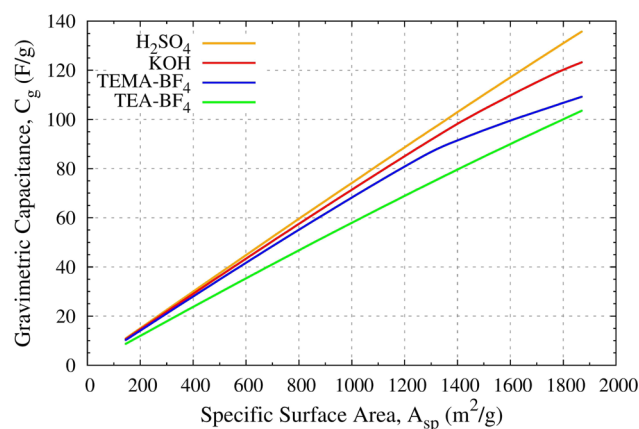
Figure 10. Comparison of the gravimetric capacitance of two organic and two aqueous electrolytes as a function of the specific surface area of the carbon electrode. The organic electrolytes are TEMA-BF$_4$ dissolved in PC and TEA-BF$_4$ dissolved in AN, while H$_2$SO$_4$ and KOH are aqueous. All electrolytes are 1 M bulk concentrations.

anions having very similar hydrated radii, permitting the use of the simplified MPB eq 5.

The two aqueous electrolyte candidates are H_2SO_4 and KOH. Just like TEMA-BF$_4$ and TEA-BF$_4$, KOH has the virtue of being binary and symmetric, cf. Table 1. However, due to the fact that the hydrated diameters of K^+ and OH^- have an appreciable difference, one must use a quarter unit cell domain and cannot use the simplified MPB eq 5.

The range of specific surface areas was attained by simulating the cell with varying pore radii, cf. eq 13. A pore radius of $r = 0.6051$ nm corresponds to a far greater number of pores and a specific surface area of $A_{sp} = 2245$ m^2/g. A pore radius of $r = 10$ nm, on the other hand, may have pores of a larger volume but far fewer of them, resulting in a lower specific surface area of $A_{sp} = 145$ m^2/g.

The overall gravimetric capacitance increases nearly linearly for the four electrolytes, especially up until $A_{sp} \sim 1300$ m^2/g. Although H_2SO_4 and TEA-BF$_4$ hold their linearity throughout the plot, TEMA-BF$_4$ and KOH have a noticeable curvature. The TEMA-BF$_4$ plot exhibits a distinct decrease in slope around $A_{sp} \sim 1300$ m^2/g.

CONCLUSION

We have developed a 3D numerical model to investigate the equilibrium behavior of EDL supercapacitors that have mesoporous activated carbon electrodes. The model is based on a modified Poisson−Boltzmann equation and can be used to determine the electrostatic potential and charge distribution within an electrochemical cell. It enables rapid parametric studies of capacitance as a function of key electrode and electrolyte parameters, notably the finite size of the ions and the field-dependent relative permittivity of the electrolyte, among others described above. A key feature of the MPB model is that it limits the accumulation of ionic charge at the electrodes based on the packing of finite sized ions. This provides more accurate predictions of device performance than models based on a point charge approximation.

We have used the model to quantify the impact of various parameters on the gravimetric capacitance. As an example, we have found that C_g is inversely proportional to hydrated ion diameter in a binary and symmetric organic electrolyte. Since the model limits the accumulation of charge to a physically realizable concentration, larger ions give rise to a lower accumulated charge at the electrode−electrolyte interface (and hence a lower capacitance), as they are less densely packed than smaller ions. Size-limited ion packing at the electrodes also explains our analysis, showing that gravimetric capacitance is relatively insensitive to variations in the bulk ion concentration. On the other hand, the capacitance was found to increase significantly with the relative permittivity ϵ_r of the electrolyte, with a higher capacitance obtained for a fixed value $\epsilon_r(0)$ as compared to a field-dependent value $\epsilon_r(E)$. This can be understood from the fact that $\epsilon_r(E)$ decreases from $\epsilon_r(0)$ as E increases in the field-dependent analysis. Thus, the lower relative effective permittivity results in a lower capacitance. The model further predicts that, for $\psi_0 > 0.1$ V, the applied voltage of the electrode is not able to accumulate charge as effectively as ψ_0 increases. This occurs from a saturation in the accumulation of ionic charge at the electrode at a low voltage, due to the finite size of the ions.

The model was also used to compare the performance of different electrolytes. Two organic and two aqueous electrolytes were investigated, and the model confirms that a higher

capacitance can be achieved with the latter. We also found that the organic TEMA-BF$_4$ and the aqueous KOH exhibit a decrease in the slope of C_g vs specific surface area near a value of 1300 m^2/g.

Finally, the model developed herein is readily implemented and computationally efficient. A parametric analysis of device performance can be completed within an hour on a modern workstation. Moreover, the model can be adapted to analyze the effects of arbitrary electrode morphologies and a broad range of electrolyte properties. It provides unique insight into the internal physics of an electrochemical cell and is well suited for the rational design of novel EDL supercapacitors.

AUTHOR INFORMATION

Corresponding Author

* E-mail: efurlani@buffalo.edu.

Notes

The authors declare no competing financial interest.

REFERENCES

(1) Burt, R.; Birkett, G.; Zhao, X. S. A Review of Molecular Modelling of Electric Double Layer Capacitors. *Phys. Chem. Chem. Phys.* **2014**, *16*, 6519−6538.

(2) Chen, T.; Dai, L. Flexible Supercapacitors Based on Carbon Nanomaterials. *J. Mater. Chem. A* **2014**, *2*, 10756−10775.

(3) Winter, M.; Brodd, R. J. What are Batteries, Fuel Cells, and Supercapacitors? *Chem. Rev.* **2004**, *104*, 4245−4270.

(4) Simon, P.; Gogotsi, Y. Materials for Electrochemical Capacitors. *Nat. Mater.* **2008**, *7*, 845−854.

(5) Wang, H.; Varghese, J.; Pilon, L. Simulation of Electric Double Layer Capacitors with Mesoporous Electrodes: Effects of Morphology and Electrolyte Permittivity. *Electrochim. Acta* **2011**, *56*, 6189−6197.

(6) Varghese, J.; Wang, H.; Pilon, L. Simulating Electric Double Layer Capacitance of Mesoporous Electrodes with Cylindrical Pores. *J. Electrochem. Soc.* **2011**, *158*, A1106−A1114.

(7) Xia, H.; Meng, S.; Yuan, G.; Cui, C.; Lu, L. A Symmetric RuO$_2$/ RuO$_2$ Supercapacitor Operating at 1.6 V by Using a Neutral Aqueous Electrolyte. *Electrochem. Solid-State Lett.* **2012**, *15*, A60−A63.

(8) Xiong, G.; Kundu, A.; Fisher, T. *Thermal Effects in Supercapacitors*; Springer International Publishing: 2015; p 147.

(9) Kim, S.-H.; Choi, W.; Lee, K.-B.; Choi, S. Advanced Dynamic Simulation of Supercapacitors Considering Parameter Variation and Self-Discharge. *IEEE Transactions on Power Electronics* **2011**, *26*, 3377−3385.

(10) Yang, L.; Fishbine, B. H.; Migliori, A.; Pratt, L. R. Molecular Simulation of Electric Double-Layer Capacitors Based on Carbon Nanotube Forests. *J. Am. Chem. Soc.* **2009**, *131*, 12373−12376.

(11) Kilic, M. S.; Bazant, M. Z.; Ajdari, A. Steric Effects in the Dynamics of Electrolytes at Large Applied Voltages. II. Modified Poisson-Nernst-Planck Equations. *Phys. Rev. E* **2007**, *75*, 021503.

(12) Kilic, M. S.; Bazant, M. Z.; Ajdari, A. Steric effects in the Dynamics of Electrolytes at Large Applied Voltages. I. Double-Layer Charging. *Phys. Rev. E* **2007**, *75*, 021502.

(13) Chapman, D. L. A Contribution to the Theory of Electrocapillarity. *Philos. Mag. Ser. 6* **1913**, *25*, 475−481.

(14) Gouy, M. Sur la Constitution de la Charge Électrique à la Surface d'un Électrolyte. *J. Phys. Theor. Appl.* **1910**, *9*, 457−468.

(15) Pham, P.; Howorth, M.; Planat-Chrétien, A.; Tardu, S. Numerical Simulation of the Electrical Double Layer Based on the

Poisson-Boltzmann Models for AC Electroosmosis Flows. *COMSOL Users Conf. 2007*, Grenoble, 2007.

(16) Helmholtz, H. Ueber einige Gesetze der Vertheilung elektrischer Ströme in körperlichen Leitern mit Anwendung auf die thierisch-elektrischen Versuche. *Ann. Phys.* **1853**, *165*, 211−233.

(17) Conway, B. E. *Electrochemical Supercapacitors: Scientific Fundamentals and Technological Applications*; Kluwer Academic/Plenum Publishers: New York, 1999; p 698.

(18) Stern, O. Zur Theorie der Elektrolytischen Doppelschicht. *Z. Elektrochem. Angew. Phys. Chem.* **1924**, *30*, 508−516.

(19) Grahame, D. C. The Electrical Double Layer and the Theory of Electrocapillarity. *Chem. Rev.* **1947**, *41*, 441−501.

(20) Gongadze, E.; Iglič, A. Decrease of Permittivity of an Electrolyte Solution Near a Charged Surface Due to Saturation and Excluded Volume Effects. *Bioelectrochemistry* **2012**, *87*, 199−203.

(21) Zou, Y.; Han, B. X. High-Surface-Area Activated Carbon from Chinese Coal. *Energy Fuels* **2001**, *15*, 1383−1386.

(22) Nightingale, E. R. Phenomenological Theory of Ion Solvation. *J. Phys. Chem.* **1959**, *63*, 508−516.

(23) Meurant, G. *Stereochemistry of Organometallic and Inorganic Compounds, Vol. 2: Stereochemical and Stereophysical Behaviour of Macrocycles*; Elsevier B.V.: Amsterdam, 2012; p 257.

(24) Hale, G. M.; Querry, M. R. Optical Constants of Water in the 200-nm to 200-μm Wavelength Region. *Appl. Opt.* **1973**, *12*, 555−563.

(25) Weast, R. C. *CRC Handbook of Chemistry and Physics*; CRC Press: 1984.